Space-time clustering of climate extremes amplify global climate impacts, leading to fat-tailed risk

Authors: Luc Bonnafous[1,2,3]*, Upmanu Lall[1,2]

Affiliations:

[1]Columbia Water Center, New York, United States

[2]Earth and Environmental Engineering Department, Columbia University, New York, United States

[3]World Bank, Washington, D.C., United States

*Correspondence to: lbonnafous@worlbank.org

Abstract: We present evidence that the global juxtaposition of major assets relevant to the economy with the space and time expression of extreme floods or droughts leads to a much higher aggregate risk than would be expected by chance. Using a century long, globally gridded time series that indexes net water availability, every year we compute local occurrences of an extreme "dry" or "wet" condition for a specified duration and return period. A global exposure index is then derived for major mining commodities, by weighting extreme event occurrence by local production exposed. We note significant spatial and temporal clustering of exposure at the global level leading to the potential for fat tail risk associated with investment portfolios and supply chains. This may not be a surprise to climate scientists familiar with the space-time patterns of inter-annual to decadal climate oscillations that can affect remote regions through teleconnections. However, the traditional approach of climate risk analysis only considers local or point extreme value analysis and hence does not account for temporal and spatial clustering of exposure for global portfolios. As multinational enterprises and supply chains assess and disclose physical climate risks, they need to consider the much higher chance that they may have multiple assets that may be exposed to extreme wet and/or dry climate extremes in the same year.

One Sentence Summary: Multinational businesses, and global supply chains can experience many more extreme climate events in a given year than would be expected by chance, due to persistent and recurrent organization in the space and time patterns of climate varaibility.

1. Introduction

A changing climate brings concerns as to whether there will be increasing business and societal disruptions as well as conflicts associated with increasing water scarcity or flooding. Even if there were no significant impact of climate change, the growing world population and

5   urbanization lead to increasing resource demands and imbalances whose changing exposure to climate risk needs to be understood. Yet, there are very few analyses *(Bonnafous, Lall, & Siegel, 2017a&b;)* of the aggregate global annual exposure to hydroclimatic extremes over the last century for specific industries, activities, or population. Given the nonstationary nature of climate extreme occurrence, and the intersection between the spatial structure of climate events

10   and the concentration of human activity, there is potential for high risk. This climate risk remains even if structural or financial instruments (e.g., insurance) were used to mitigate it at each location, as is the norm. Typically, these instruments are designed based on the prior local climate record. Sometimes local information on local climate cycles (see for instance (Khalial, Kwon, Lall, Miranda, & Skees, 2007) or non-stationarity in event modeling (e.g. (Lima, Lall,

15   Troy, & Devineni, 2015), (Hanel, Bruishand, & Ferro, 2009)) is used. The implication at the portfolio level could be a fat tailed, systemic risk for global enterprises.

From the perspective of a global investor, or of a development or humanitarian aid agency, an assessment of the potential occurrence of many extreme hydroclimatic events across the planet in

20   a given year is needed to assess potential supply chain risks, production shortfalls, conflict or needs for humanitarian relief. The World Bank noted that its development efforts can be compromised by climate extremes and climate change *(World Bank, 2014)*. The 2011 floods in Thailand, the 2010 floods in Queensland and Pakistan, the 2014-16 drought in Sao Paolo, and the

2016-18 drought in Cape Town drew attention from their supply chain risk implications as well as the potential for the disruption of tourism, and global business. An area where the impacts of climate risk on global production has been highlighted is agriculture *(USDA, 2010; Piao et al., 2010)*. Drought led to restrictions on exports of rice from key producing countries in 2008,

5 leading to a doubling of the global price *(Slayton, 2009; Bradsher, 2008)*. In this paper, we focus on another area of the economy, mining, but also show some results for urban areas and four major crops as a reference in the supplementary material. We consider global socio-economic exposure to the nominal once in 10 year local hydroclimate extreme for the annual production of four major mining commodities (using 2014 and 2013 production data) *(SNL, 2016)* at the major

10 mining locations, that represent a significant part (between 53 and 78%) of global production,. Both dry and wet events are considered for mining given the potential additional expense on water sourcing in a drought, and mine dewatering in wet years. The intention is to illustrate the nature of global exposure using a few globally relevant commodities.

2. Data and Methods

The evolution through time of wet and dry extremes has primarily been studied through indices derived directly from precipitation (P) time series, and through relationships between P, evapotranspiration (E), potential evapotranspiration (E_p), soil moisture (SM), runoff (R) and drought indices such as the Palmer Drought Severity Index (PDSI) and the Standardized

20 Precipitation-Evapotranspiration Index (SPEI). The SPEI *(Beguería, Vicente-Serrano, & Angulo-Martínez, 2010; Beguería, Vicente-Serrano, Reig & Latorre, 2014)* is a scalar index reported monthly. It is built after fitting a distribution on the cumulative $P - E_p$ over a window of interest (e.g., 12 months). The dataset used is based on Climate Research Unit (CRU) *(Harris, Jones, Osborn & Lister, 2014)* data for both precipitation and potential evapotranspiration and is

accessible at http://spei.csic.es/database.html. CRU is a gridded dataset with 0.5° x 0.5° spatial

resolution of monthly temperature and precipitation built using interpolation of station network

data, itself accessible at https://crudata.uea.ac.uk/cru/data/hrg/). The SPEI is thus a measure of

the net water supply, as estimated using local precipitation and potential evapotranspiration, over

specified durations. We chose to use the SPEI for our analysis since a global reconstruction of

this index covering 1901-2014 that has been well verified was available, at a grid resolution of

0.5°. Since we are interested in an annual exposure, we used the 12-month duration values of the

SPEI. We limit our analyses to the land area bounded by 60°S to 60°N, and retain grid blocks

that have no more than 10% missing data. To define a dry (wet) event, we first record, for each

year, at each site, the quantile of SPEI time series for the return-level of interest (e.g. for a 10-

year return level, on the dry side, the threshold is defined as $quantile(SPEI_{yr}^{min}, 0.1)$, while on

the wet side it will be $quantile(SPEI_{yr}^{max}, 0.9)$. Months for which the SPEI is below (above)

these thresholds are marked as belonging to a dry (wet) event. It should be noted that CRU may

not provide adequate spatial coverage far back in time, especially in the Southern Hemisphere.

This may affect the SPEI. For our first analysis, we consider the global land area exposed. Each

event is then weighted by the area of the grid-block it corresponds to divided by the total land

area. Further, using CRU data, we consider extremes in P and E_p: for both of these variables, we

aggregate monthly values over 12-month windows and define wet and dry events at a given

location as above (inversing thresholds for E_p). In the supplementary material (**Fig. S18**), we

also compare the results with those based on data from the NOAA's 20th Century Reanalysis

(20CR) project *(Compo et al., 2011)*, accessible here:

https://www.esrl.noaa.gov/psd/data/gridded/data.20thC_ReanV2c.html (the variable names are "prate" for

precipitation and "pevpr" for potential evapotranspiration) . We use the P and E_p data of 20CR

to compute a version of the SPEI. In each case, we study the proportion of the area of the world affected by dry or wet, dry, wet and dry and wet events in a given year.

Production data is collected from *(SNL, 2016)* to find the location of producing bauxite, copper,

5   gold and iron ore copper mines in 2014. Each climate event is then weighted with the 2014 share of production of each mine.

Wavelet and multitaper spectral analyses were performed to assess cycles in the exposure time series and their covariation patterns with climate indices. Using package biwavelet *(Gouhier,*

10   *Grinsted, & Simko, 2016)*, we investigate the spectra and the coherence across series. Spectra are also assessed using multitaper analysis *(Rahim, Burr & Rahim, 2017)*.

3. Results

The key findings from our analyses are illustrated in **Fig. 1** and **2**. We use the 1901-2014 data of the SPEI12 index, thus a measure of net water availability based on the cumulative difference

15   between precipitation and potential evapotranspiration for a 12 month duration at each location, which is computed for each month in the record, and then mapped to a probability distribution, yielding monthly time series. We consider the 90th (10th) percentile of yearly maximum (minimum) of the SPEI time series at each location as a "dry" ("wet") threshold, corresponding to a 10 year return period event. The exceedance of this threshold at a given location in each year

20   of the climate record is then weighted by the production (assumed here to be constant) at that location and spatially aggregated to provide an estimate of annual exposure.

In the worst year, nearly 40% of the global land area experienced a 10-year dry or a wet event. Sectoral impacts are heavily clustered when assets are concentrated in a few locations. This is for

instance the case for phosphates, for which, the worst year translated into a nearly 84% exposure of global production, or for lithium and lead. Nearly 50% of global copper production is exposed to a dry or wet event, in the worst year of available data. For each of the portfolios considered, the worst exposure in the record, has a negligible probability of occurrence if one were to consider the local 10 year return period events occurring independently and randomly over the earth. We assessed these probabilities using 100,000 simulations of the 114 year record assuming the same asset values at each mining site, and random sampling of hit or no hit independently at each location using the local marginal probabilities for the events. . This illustrates that the spatial concentration of risk across the earth is dramatic for the tail events, highlighting the potential for multiple hits at the global scale a few years per century, much more frequently than may be expected by chance considering locations independent from each other. If, for a given commodity i, we call X_i the production exposed in a given year, and M_i the maximum share of production exposed observed over 114 years, we have the following table:

Table 1: Share of global commodity portfolios exposed to wet and dry events. M_i is the maximum share of production exposed observed over 114 years. $pexc(M_i)$ refers to the probability that this level of exposure or higher could occur across the different mining sites if the climate risks were not spatially correlated.

Commodity i	Share of world production in the database	M_i	$pexc(M_i)$
Bauxite	0.63	0.65	0.1865
Copper	0.78	0.50	0
Gold	0.61	0.42	0
Iron Ore	0.53	0.69	0

Density estimation (**Fig.1**) also highlights the potential for fat tails, while smoothed time series of exposure with a smoothing window of 11 years (**Fig. 2**), make evident the existence of cycles.

Empirical and simulated logspline density estimation of the exposure of the bauxite portfolio

Empirical and simulated logspline density estimation of the exposure of the copper portfolio

Empirical and simulated logspline density estimation of the exposure of the gold portfolio

Empirical and simulated logspline density estimation of the exposure of the iron portfolio

Fig. 1: Empirical (red) and i.i.d. process simulated (grey) density estimation of the yearly share of global production exposed to a wet or dry 10-year event according to the 12-months SPEI for four different portfolios

25
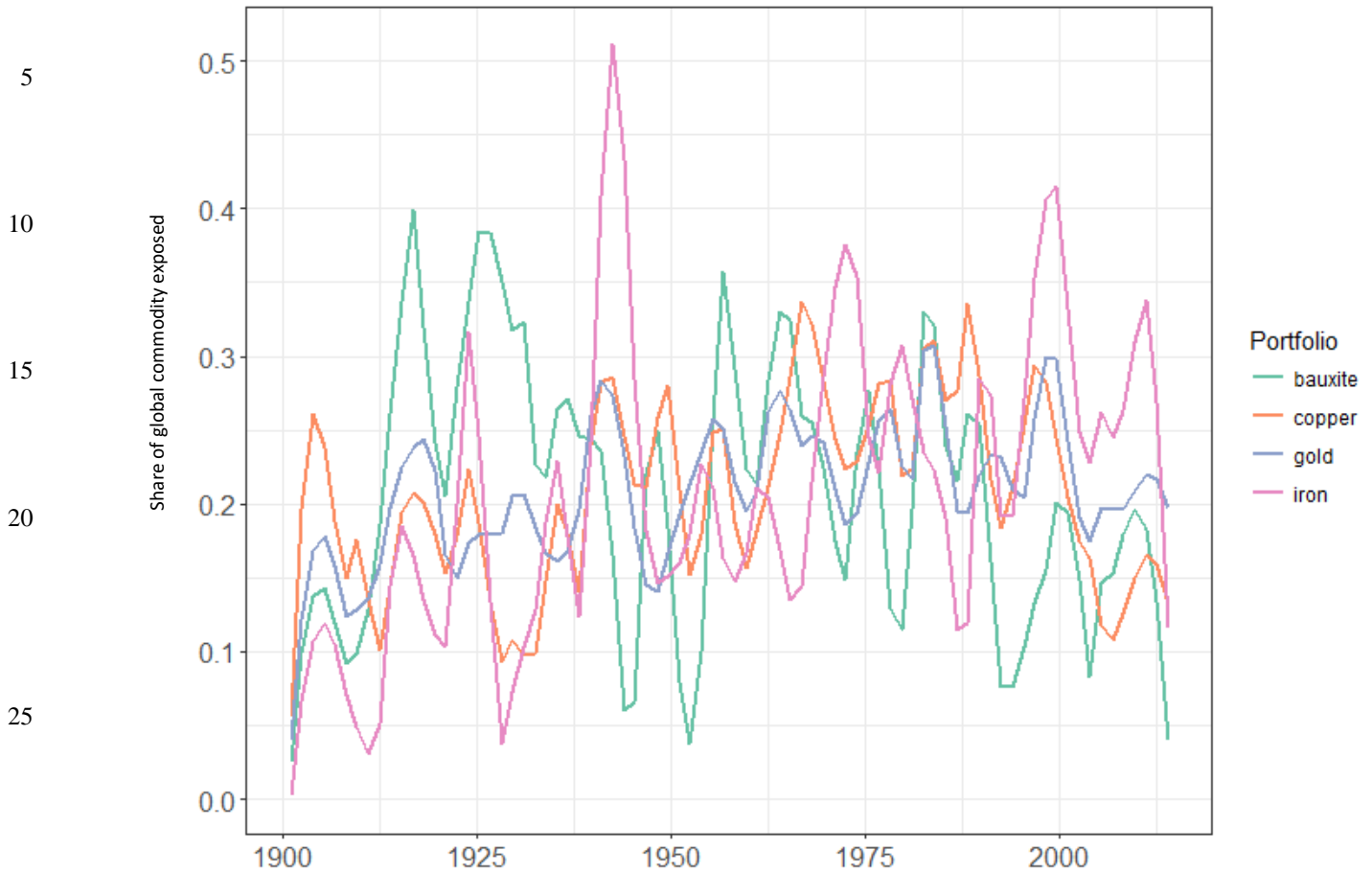
Fig. 2: Time series of weighted global annual share of production exposed for different commodities with 11 year local regression smoothed trends. Wet and dry events are considered

Consistent with many analyses of longer duration hydrologic extremes *(Greve et al., 2014; Sheffield & Wood, 2008; Sippel et al., 2017; Trenberth et al., 2014),* the time series of global annual exposure for mining reveals a cyclical rather than monotonically increasing or decreasing trend (as may be expected from anthropogenic climate change). In several of the cases, using wavelet and spectral analyses we find evidence for connections to the El Niño Southern Oscillation and to climate indices known to exhibit decadal variability (**Fig. S9-S13**).

Given these observations, we explored the global land area exposed. The temporal trend of the
global land area exposed to the crossing of the dry and wet thresholds of the 12 month SPEI
index is shown in **Fig. 3.** An increase in the area affected by events of all types occurred through
the 1970's. This was followed by a decrease in the total affected area. Note that the threshold

5   used to determine whether an extreme event occurred at a location or not is determined as the
appropriate quantile at that location using the corresponding data source. Hence, generic biases
in observations in the net water availability at any location are not an issue in determining
whether or not an extreme event occurred.
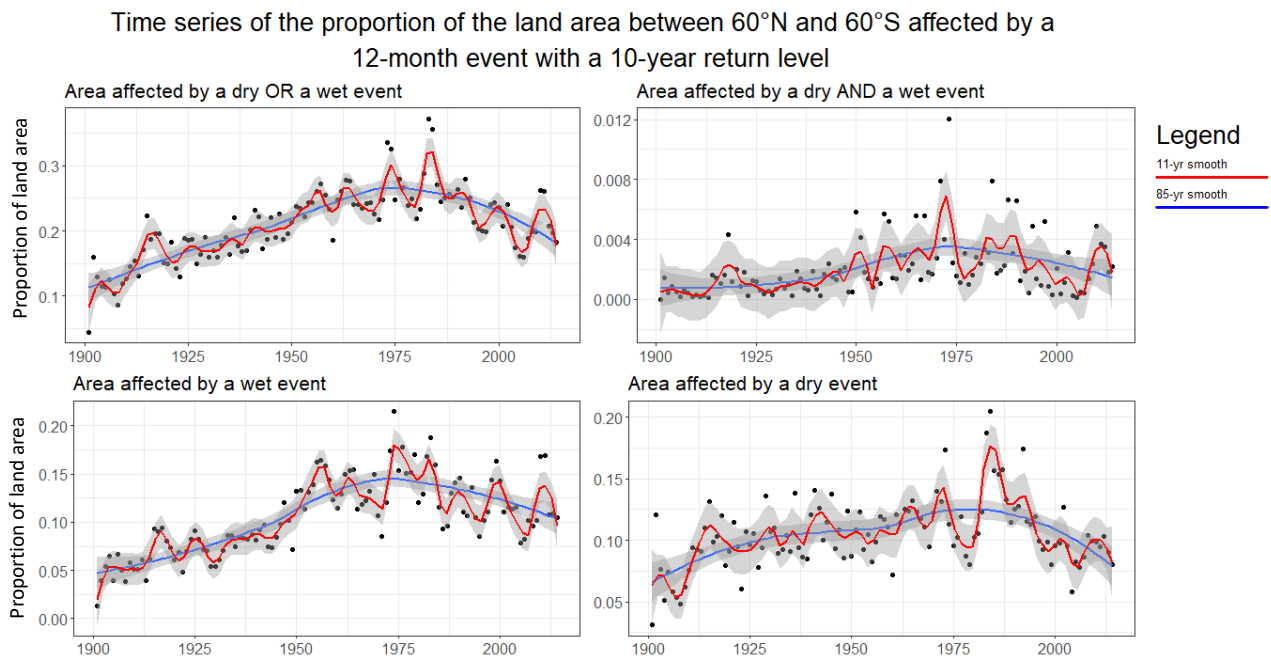
Fig. 3: Global area proportion affected annually by exceedance of the 10-year, 12-month SPEI index for wet or dry (top left), wet

20   *and dry (top right), wet (bottom left), and dry areas (bottom right) event, with 95th confidence interval in shaded grey.*
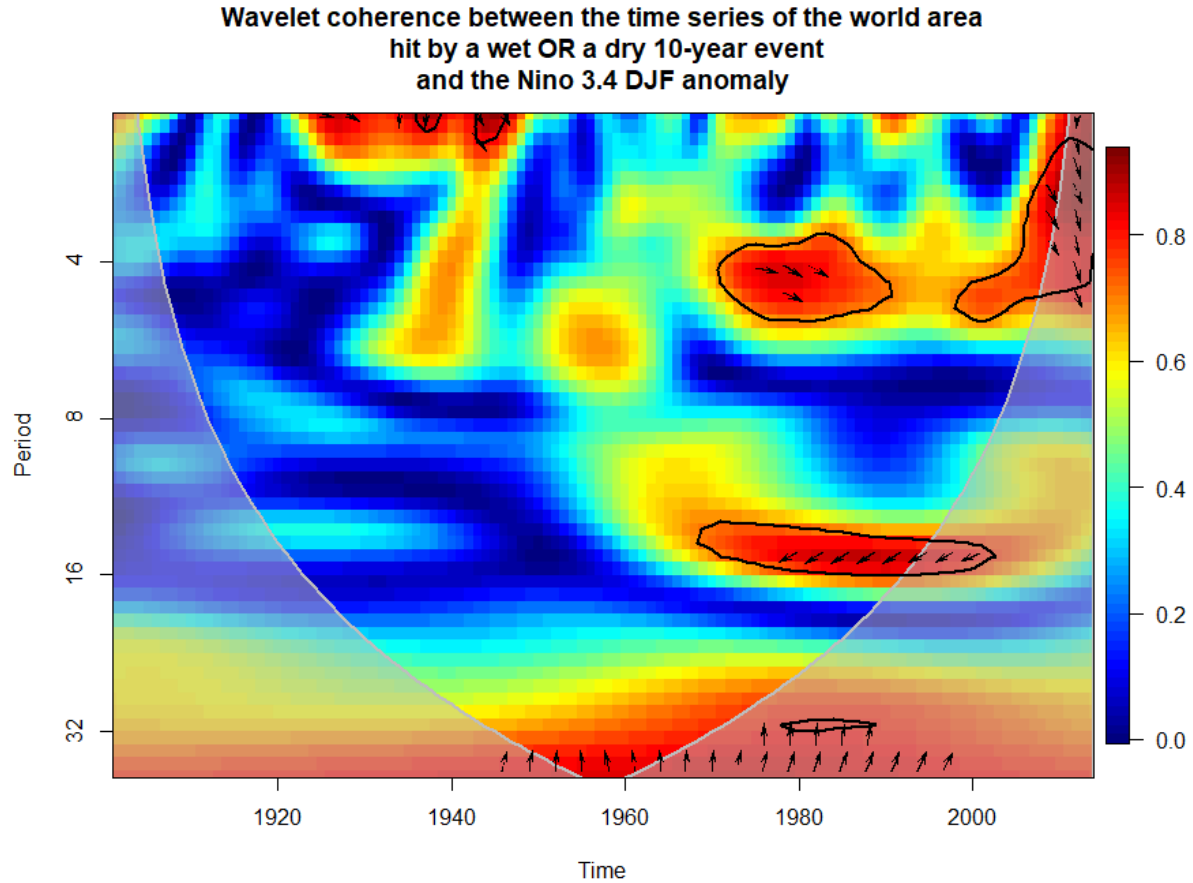
Figure 4: Wavelet coherence between the global share of area exposed and the Nino 3.4 DJF anomaly. The arrow directions indicate the phase (0 degrees is concurrent, 180 deg is perfectly out of phase) of the relationship between exposure and NINO3.4 for frequency bands and times when the coherence is statistically significant, as marked by the black encircled areas. The gray shaded zone indicates areas with edge effects that preclude a robust identification of significance given the combination of the sample size and the period of the oscillation.

The recent decrease in wet events is largely observed in the tropics and subtropics for the CRU data (**Fig. S7**). The 1982-1983 El Niño event corresponds to the highest number of extremes (**Fig. 3, Fig.5**). The 5 years that show up with most events are (in decreasing order): 1983, 1984, 1973, 1974, and 1976. Except for 1984, these correspond to some of the strongest December-January-February (DJF) El Nino Southern Oscillation (ENSO) conditions (El Niño for 1983, 1973, La Niña for 1974 and 1976) *(NOAA ESRL, 2016)*. Wavelet analyses of the derived hit series (performed with biwavelet *(Gouhier, Grinsted, & Simko, 2016)* show significant inter-

annual and decadal variations, and are coherent with the NINO3.4 index at interannual (4 years) and decadal (16 years) frequencies after 1970 (**Fig. 4**

). Coherence is characterized by warmer colors, with significant regions circled in black. A Multitaper spectral analysis *(Rahim, Burr, & Rahim, 2017; Slepian, 1978; Thomson, 1982)* also shows coherence for cycles of 4 years, consistent with the ENSO and North Atlantic Oscillation (NAO) phenomena (**Fig. S14,** where common oscillatory behaviors from multitaper analysis are marked by spikes with the x axes corresponding to cycles/year; thus a 0.2 value corresponds to 5-year cycle), and with the Pacific Decadal Oscillation (PDO) index at scales of about 8 years.
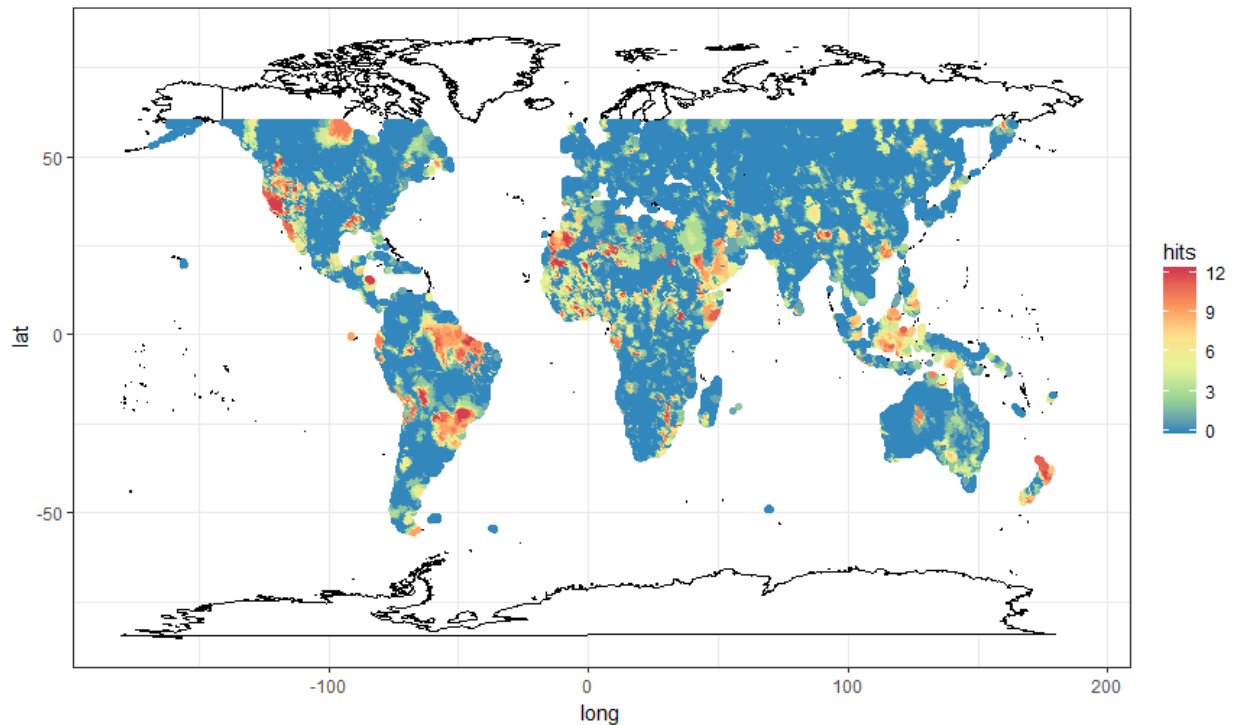
Figure 5: Map of the number of months in exceedance of a 10-year return level threshold for a wet or dry event in 1983. Here each month that was exceeding either the wet or dry 10-year return level threshold counts as a "hit".

The spatial teleconnections of hydrologic extremes to the El Niño Southern Oscillation, and other organized modes of inter-annual to decadal climate variability are well studied and their impacts on agriculture and disasters are documented *(Rojas, Li, & Cumani, 2014)*. However,

other than studies on the production of specific crops, an analysis of the impact of these climate modes on the aggregate global impact has not been previously done, especially considering a specific risk threshold.

4. **Conclusion**

In prior work *(Bonnafous, Lall, & Siegel, 2017a&b)* we illustrated impacts of hydrologic extremes with different return periods on mining company portfolios, and the associated potential value at risk. For global companies and supply chains, the role of hydroclimatic risk clustering in space and time is not well studied, especially since the exposure could result from a combination of effects on real assets, transportation, energy, water and health infrastructure, production and increase in local conflict under drought. A first step would be to develop influence diagrams that reflect the pathways of climate exposure for an investment portfolio or supply chain, and then integrate social and economic factors to assess possible aggregate exposure. Critical path analyses on these exposure networks can then be performed to identify exposure pathways that contribute most significantly to the aggregate risk, and to then develop risk mitigation strategies for those pathways. Such a framework would take into account compound events, and simply "add" the space-time clustering of risk to a framework akin to the one advocated in *(Zscheischler et al., 2018)*. Examples of industry asset portfolios that could benefit from such analysis include (but are not limited to) renewable energy production facilities (e.g. dams for floods and droughts, windmills for extreme winds or low-wind periods), or transport infrastructure such as ports. Agriculture is a particular case, as much work has been done on it and would need to be properly integrated in the framework, for instance regarding the regional spatial extent and timing of droughts.

A question that arises once people understand the global portfolio level risk due to the space-time correlation of exposure, is how can someone who is exposed to such risk manage it? Examples of groups that could be exposed include a) the World Food Program, that provides food aid to regions that need it post drought or flood losses; b) Energy companies that are concerned with a disruption in the copper or lithium supply chain, and associated shortages and price increases; and c) multi-national insurance companies faced with business interruption claims or correlated draws for payments. Parametric insurance and related financial instruments could provide an effective approach for risk mitigation in such cases. Examples of such products indexed to ENSO indices are available at scales ranging from farmer and micro-insurance to national banks to the World Food Program *(Khalil, Kwon, Lall, Miranda, & Skees, 2007; Carriquiry & Osgood, 2012; Hellmuth, Osgood, Hess, Moorhead, & Bhojwani, 2009)*. Consider that a product were available where one could purchase a unit of insurance against a climate index (e.g., ENSO) exceeding a specified threshold, and the historical data for the index were publicly available. Then, a global or regional portfolio manager concerned with aggregate risk exposure could explore how often an exceedance of that threshold also led to an exceedance of the risk threshold for each element on their own exposure pathway, and assess how well that index would influence their aggregate risk exposure. Where multiple climate indices are available for parametric insurance, the manager could optimize their allocation to a combination of those indices to mirror their risk exposure. Tradeoffs via reduction in exposure by considering alternate suppliers or by structural measures (e.g., storage or inventory) could also be considered.

Arguably, the SPEI provides a version of net precipitation and is advocated as a drought index.

Indeed, for runoff, considerably more complex dynamics matter, but accurately modeling

flooding risk at the asset scale globally is still confounded by considerable uncertainty.

Our intention here is to highlight the space-time clustering of the wet/dry risks for different

5   sectors and not to model these effects at the asset scale. For this purpose, we considered the tail

events of the long record of the SPEI to be useful. We did not consider the application of the

state of the art probabilistic drought and flood model at high spatial resolution globally to be

necessary to make the same point. The uncertainty associated with the climatic and soils data and

the lack of calibration/verification data from the application of such models may not justify the

10   additional effort if the point to be made was one of the nature of space and time variation of

climate and its implication for risk.

On one hand, the quality of historical climate data sets degrades especially as one goes back

before 1950. On the other hand, climate re-analysis products as well as the IPCC climate model

15   integrations for the 20th century are known to show significant biases for hydroclimatic variables

(Bozkurt, Rojas, Boisier, & Valdivieso, 2017; Ficklin, Abatzoglou, Robeson, & Dufficy, 2016;

Liu, Mehran, Phillips, & AghaKouchak, 2014). However, we expect the conclusion as to the

space and time clustering that translates into a fat tailed risk for global enterprises is robust.

On the other hand, one might advocate that the datasets used here may not fully represent

20   extremes, especially on the wet side, as complex dynamics such as runoff conditions and

hydrological routing are involved at the local level. However, accurately modeling flooding risk

at the asset scale globally is still confounded by considerable uncertainty associated with the

climatic and soils data and the lack of calibration/verification data from the application of state-

of-the-art hydrological models. Plugging such a model in our approach is obviously feasible and could be part of a larger effort including exploring the risk-level space. Our goal was here to highlight that currently the space-time correlation structure of climate risk at the global scale due to quasi-periodic planetary scale climate regimes is largely unaddressed by risk managers, and to

5   establish the need to do so, retrospectively and prospectively. Analyses of the biases and uncertainty attendant to future climate projections in this context are needed and will depend on the model and the space-time resolution of the analysis.

Code/Data availability

Datasets are available at the links provided and upon request. Codes are available upon request.

10   **Author contributions**

Luc Bonnafous performed participated in designing the study, writing the paper and produced the analysis

Upmanu Lall participated in designing the study and writing the paper

Competing interests

15   The authors declare that they have no conflict of interest.

Beguería, S., Vicente-Serrano, S. M., & Angulo-Martínez, M. (2010). A multiscalar global drought dataset : The SPEI base : A new gridded product for the analysis of drought variability and impacts. *Bulletin of the American Meteorological Society*, *91*(10), 1351-1356. https://doi.org/10.1175/2010BAMS2988.1

20   Beguería, S., Vicente-Serrano, S. M., Reig, F., & Latorre, B. (2014). Standardized precipitation evapotranspiration index (SPEI) revisited : Parameter fitting, evapotranspiration models, tools, datasets and drought monitoring. *International Journal of Climatology*, *34*(10), 3001-3023. https://doi.org/10.1002/joc.3887

Bonnafous, L., Lall, U., & Siegel, J. (2017a). An index for drought induced financial risk in the mining industry. *Water Resources Research*, *53*, 1-23. https://doi.org/10.1002/2016WR020339.Received

Bonnafous, Luc, Lall, U., & Siegel, J. (2017b). A water risk index for portfolio exposure to climatic extremes : Conceptualization and an application to the mining industry. *Hydrology and Earth System Sciences*, *21*(4), 2075-2106. https://doi.org/10.5194/hess-21-2075-2017

Bozkurt, D., Rojas, M., Boisier, J. P., & Valdivieso, J. (2017). Climate change impacts on hydroclimatic regimes and extremes over Andean basins in central Chile. *Hydrology and Earth System Sciences Discussions*, (January), 1-29. https://doi.org/10.5194/hess-2016-690

Bradsher, K. (2008). A Drought in Australia, a Global Shortage of Rice. *New York Times, 17 Apr 2008*, Vol. 2018.

Carriquiry, M. A., & Osgood, D. E. (2012). Index Insurance, Probabilistic Climate Forecasts, and Production. *Journal of Risk and Insurance*, *79*(1), 287-300. https://doi.org/10.1111/j.1539-6975.2011.01422.x

Compo, G. P., Whitaker, J. S., Sardeshmukh, P. D., Matsui, N., Allan, R. J., Yin, X., … Worley, S. J. (2011). The Twentieth Century Reanalysis Project. *Quarterly Journal of the Royal Meteorological Society*, *137*(654), 1-28. https://doi.org/10.1002/qj.776

Ficklin, D. L., Abatzoglou, J. T., Robeson, S. M., & Dufficy, A. (2016). The influence of climate model biases on projections of aridity and drought. *Journal of Climate*, *29*(4), 1369-1389. https://doi.org/10.1175/JCLI-D-15-0439.1

Gouhier, A. T. C., Grinsted, A., & Simko, V. (2016). Package « biwavelet ». *CRAN*, 1-38.

Greve, P., Orlowsky, B., Mueller, B., Sheffield, J., Reichstein, M., & Seneviratne, S. I. (2014). Global assessment of trends in wetting and drying over land. *Nature Geoscience*, *7*(10), 716-721. https://doi.org/10.1038/NGEO2247

Harris, I., Jones, P. D., Osborn, T. J., & Lister, D. H. (2014). Updated high-resolution grids of monthly climatic observations—The CRU TS3.10 Dataset. *International Journal of Climatology*, *34*(3), 623-642. https://doi.org/10.1002/joc.3711

Hellmuth, M. E., Osgood, D. E., Hess, U., Moorhead, A., & Bhojwani, H. (2009). Index insurance and climate risk : Prospects for development and disaster management. In *Prospects* (Vol. 2).

Jain, S., & Lall, U. (2001). Floods in a changing climate : Does the past represent the future? *Water Resources Research*, *37*(12), 3193-3205. https://doi.org/10.1029/2001WR000495

Khalil, A. F., Kwon, H. H., Lall, U., Miranda, M. J., & Skees, J. (2007). El Niño-Southern Oscillation-based index insurance for floods : Statistical risk analyses and application to Peru. *Water Resources Research*, *43*(10), 1-14. https://doi.org/10.1029/2006WR005281

Liu, Z., Mehran, A., Phillips, T. J., & AghaKouchak, A. (2014). Seasonal and regional biases in CMIP5 precipitation simulations. *Climate Research*, *60*(1), 35-50. https://doi.org/10.3354/cr01221

NOAA ESRL. (2016). TOP 24 STRONGEST EL NIÑO AND LA NIÑA EVENT YEARS BY SEASON.

Piao, S., Ciais, P., Huang, Y., Shen, Z., Peng, S., Li, J., … Fang, J. (2010). The impacts of climate change on water resources and agriculture in China. *Nature*, *467*(7311), 43-51. https://doi.org/10.1038/nature09364

Rahim, A. K., Burr, W. S., & Rahim, M. K. (2017). *Package ' multitaper '*.

Rojas, O., Li, Y., & Cumani, R. (2014). *An assessment using FAO's Agricultural Stress Index (ASI) Understanding the drought impact of El Niño on the global agricultural areas :* https://doi.org/10.13140/2.1.1868.3687

Sheffield, J., & Wood, E. F. (2008). Global trends and variability in soil moisture and drought characteristics, 1950-2000, from observation-driven simulations of the terrestrial hydrologic cycle. *Journal of Climate*, *21*(3), 432-458. https://doi.org/10.1175/2007JCLI1822.1

Sippel, S., Zscheischler, J., Heimann, M., Lange, H., Mahecha, M. D., Jan Van Oldenborgh, G., … Reichstein, M. (2017). Have precipitation extremes and annual totals been increasing in the world's dry regions over the last 60 years? *Hydrology and Earth System Sciences*, *21*(1), 441-458. https://doi.org/10.5194/hess-21-441-2017

Slayton, T. (2009). Rice Crisis Forensics : How Asian Governments Carelessly Set the World Rice Market on Fire. *Development*, (163), 43. https://doi.org/10.2139/ssrn.1392418

Slepian, D. (1978). Prolate spheroidal wave functions, Fourier analysis, and uncertainty. V-The discrete case. *ATT Technical Journal*, *57*(5), 1371-1430. https://doi.org/10.1002/j.1538-7305.1978.tb02104.x

SNL. (2016). *SNL Mining and Metals database*.

Thomson, D. J. (1982). Spectrum estimation and harmonic analysis. *Proceedings of the IEEE*, *70*(9), 1055-1096. https://doi.org/10.1109/PROC.1982.12433

Trenberth, K. E., Dai, A., Van Der Schrier, G., Jones, P. D., Barichivich, J., Briffa, K. R., & Sheffield, J. (2014). Global warming and changes in drought. *Nature Climate Change*, *4*(1), 17-22. https://doi.org/10.1038/nclimate2067

USDA. (2010). Effects of the Summer Drought and Fires on Russian Agriculture. *USDA GAINS report*, *RS1061*.

Vicente-Serrano, S. M., Beguería, S., López-Moreno, J. I., Angulo, M., & El Kenawy, A. (2010). A New Global 0.5° Gridded Dataset (1901–2006) of a Multiscalar Drought Index : Comparison with Current Drought Index Datasets Based on the Palmer Drought Severity Index. *Journal of Hydrometeorology*, *11*(4), 1033-1043. https://doi.org/10.1175/2010JHM1224.1

World Bank. (2014). *Turn Down the Heat : Confronting the New Climate Normal*. Consulté à l'adresse World Bank website: https://openknowledge.worldbank.org/handle/10986/20595

Zscheischler, J., Westra, S., Hurk, B. J. J. M. Van Den, Seneviratne, S. I., Ward, P. J., Pitman, A., AghaKouchak, A., Bresch, D. N., Leonard, M., Wahl, T., Zhang, X., (2018). Future climate risk from compound events. *Nature Climate Change*, (May). https://doi.org/10.1038/s41558-018-0156-3

Acknowledgments

Support for the Twentieth Century Reanalysis Project version 2c dataset is provided by the U.S. Department of Energy, Office of Science Biological and Environmental Research (BER), and by the National Oceanic and Atmospheric Administration Climate Program Office